

Pattern Recognition of the Seismic Demands for Tall Pier Bridge Systems

Farahnaz Soleimani

To cite this article: Farahnaz Soleimani (2021): Pattern Recognition of the Seismic Demands for Tall Pier Bridge Systems, Journal of Earthquake Engineering, DOI: [10.1080/13632469.2021.1927894](https://doi.org/10.1080/13632469.2021.1927894)

To link to this article: <https://doi.org/10.1080/13632469.2021.1927894>



Published online: 31 May 2021.



Submit your article to this journal [↗](#)



Article views: 54




View related articles [↗](#)



View Crossmark data [↗](#)



Pattern Recognition of the Seismic Demands for Tall Pier Bridge Systems

Farahnaz Soleimani 

Department of Civil and Environmental Engineering, Georgia Institute of Technology, Atlanta, GA, USA

ABSTRACT

An essential and emerging task in the area of performance-based seismic assessment of bridges is to improve the estimation of the seismic demands. Existing research proved that the bridge column is one of the dominant components in estimating the bridge system vulnerability. However, the seismic performance of bridges with tall piers is not deeply investigated yet. This study aims to address this problem through analysis of multi-span concrete box-girder bridges with tall piers. This study implements a clustering algorithm that identifies optimized groupings which can set up the basis to establish the best choice for generating MLPSDMs. The evaluation results implicate better performance of cluster-wise multiple models than a single model to represent the variation in the bridge demands. The insights gained from the findings of this study can pave the way toward a better realization of the seismic performance of bridges having tall piers.

ARTICLE HISTORY

Received 30 March 2020
Accepted 2 May 2021

KEYWORDS

Tall piers; seismic demand; box-girder concrete bridges; probabilistic seismic analysis; pattern recognition; clustering analysis; bridge vulnerability

1. Introduction

Topography specifications do not always allow bridge constructions to follow standard guidelines, and modifications are required to accommodate the particular needs of individual landscapes (Soleimani 2017). As a result, in challenging regions such as mountain areas and regions with deep valleys, bridges end up having taller piers than those commonly used in bridges that are located in ordinary terrains (Zheng and Liu, 2010). Inferred from damage detection during post-earthquake investigations (Buckle 1994; Kawashima et al. 2010; Yashinsky et al. 2010), bridges with unconventional configurations or characteristics are more prone to experiencing deterioration. Although extensive research explored the nonlinear behavior of normal concrete bridges subjected to earthquakes (Abdel-Mohti and Pekcan 2008; Button, Cronin, and Mayes 2002; Kawashima and Mizoguti 2000; Lee et al. 2011; Liang, Mosalam, and Günay 2016; Padgett and DesRoches 2007; Simon, Bracci, and Gardoni 2010; Soleimani et al. 2016; Soleimani et al., 2017d; Zhang et al. 2003), there exist limited studies evaluating the unique dynamic characteristics of bridges with tall piers.

As an example, Chen et al. (2018) tested the seismic behavior of two 1/7-scale tall concrete columns constructed in China. During the shake table test, the near-fault Rinaldi ground motion selected from the 1994 Northridge earthquake was applied on two specimens in which one had a lumped mass on the cap and the other column had a distributed mass applied along the pier height. Despite the typical assumption of elastic behavior of columns at the midpoint, they found a plastic region around the mid-height of the specimens. Revising the seismic design codes of tall piers to increase the reinforcement and confinement ratios around the column's mid-height was suggested to address this concern and to enhance the column's ductility. In addition, Chen et al. (2020) conducted shake table tests on tall pier specimens to identify significant ground motion features for developing fragility curves of the

columns. They concluded that, for near-fault pulse-like motions, fragility values are sensitive to the ground motion period.

Kulkarni et al. (2016) assessed the seismic performance of a five-span railway bridge with steel trusses superstructure and tall concrete piers located at the central span of the bridge. They performed nonlinear static pushover and nonlinear dynamic analysis. Although elastic behavior was observed in the tall piers of the most considered bridges, bridge columns experienced significant displacement at the top. They also noticed that the seismic performance of these types of piers is sensitive to the foundation–soil interaction and the P - Δ effect. Since the mid-height plastic hinge was not detected by the static pushover analysis, it was concluded that performing nonlinear dynamic analysis is a required step in the seismic evaluation of tall piers.

Falamarz-Sheikhabadi and Zerva (2017) investigated the seismic response of a long three-span, curved, reinforced concrete bridge with flared tall columns subjected to nine seismic excitations chosen from Loma Prieta, Northridge, San Fernando, and N. Palm Springs earthquakes. They used various methodologies for numerical modeling and analysis including incremental dynamic analyses, nonlinear static pushover, and time history analysis. The sensitivity study of the bridge responses to the modeling strategies revealed that static pushover analysis is not enough to capture the real behavior of the considered bridge. The critical behavior of the columns was observed while applying uniform excitations to the bridge. In addition, the flared designed columns (Soleimani 2017a) could increase the flexural capacity of the columns and restrict the torsional movement of the bridge deck.

Soleimani (2017) proposed a simplified approach to modify the probabilistic seismic demand models of irregular bridges including skew angle, tall piers, and unbalanced stiffness frame. The modified probabilistic seismic demand models (PSDMs) reduce computational costs in generating demand models as well as the fragility curves. Based on the comparison of the fragility values obtained from the analyses of tall bridges and normal box-girder bridges, it was found that tall bridges are more prone to experience damage at the same level of intensity measure. Likewise, through the fragility analysis, Mangalathu et al. (2018) found that the increase in the column height increases the bridge vulnerability. They investigated a horizontally curved concrete box-girder bridge with two frames, five spans, and single-column bents. In agreement with research on the effect of superstructure curvature on the seismic performance of box-girder bridges (e.g., Soleimani 2017b), they indicated a direct correlation between the increase in the bridge vulnerability and the radius of curvature.

Based on the bridge portfolio, various bridge characteristics could influence the overall seismic evaluation of the system (Mangalathu, Soleimani, and Jeon 2017b; Mangalathu et al. 2017a). To this end, researchers explored the sensitivity of the seismic demands and system fragility of bridges. Chen (2020) focused on tall bridges with T-girder superstructure commonly constructed in Southwest China. The studied class of bridge, which had two piers and variable hollow sections, was subjected to near-fault ground motions. Component fragility curves were derived for the pier column and rubber bearing which were combined to generate the bridge system fragility curves. For the studied bridge type, it was found that the rubber bearings dominated the system fragility curve. Soleimani et al. (2017c) conducted statistical analyses to detect a combination of features notably influencing the seismic response of concrete box-girder bridges. Bridge column parameters including the column height and reinforcement ratios were identified and ranked as the most influential features. Moreover, Soleimani (2020) measured uncertainties associated within the process of probabilistic seismic evaluation of tall concrete bridges. It was shown that the majority of response variability was caused by the geometric random variables used to create bridge sampling.

These works imply the necessity of extending seismic evaluation of tall bridges to improve the understanding of the distinctive behavior of this class of bridges. In this regard, the current paper aims to realize the seismic performance of bridges consisting of tall piers by performing nonlinear time history analyses of multi-span concrete box-girder bridges, extracting seismic demands, and conducting statistical inspections of the bridge responses. To properly take into account the uncertainties associated within the seismic evaluation procedure, both deterministic and probabilistic analyses are

conducted, and the discrepancies in the bridge responses are highlighted. Besides, a set of clustering algorithms is implemented to determine the inherent variety and grouping hidden in the collected data. In fact, the findings of this study help to better realize the pattern prediction and evaluation of seismic behavior of bridges with tall columns.

More recent studies (e.g., Du and Padgett 2019; Pang, Dang, and Yuan 2014) indicated that the classical probabilistic seismic demand models may not be suitable for all bridge types. The classical models are based on the assumption of lognormally distributed demands and a linear relationship between the peak responses of bridge components, subjected to excitations, and the ground motion intensity. Thereby, a single linear regression model is typically fitted to the seismic demands and intensities in the logarithmic space. In the seismic performance evaluation of bridges, a wide range of uncertainties originating from modeling and ground motion parameters are involved which creates inevitable variability in the simulated demands. This variability can be exacerbated for a bridge with irregular configurations such as tall bridges since additional sources of uncertainties are engaged in their analysis (Soleimani 2021). In fact, this is particularly more noticeable in the case of probabilistic performance analysis. As a result, the classical single linear model may not be able to efficiently capture the variability in the responses for all bridge types. This study provides an alternative approach to produce demand models that similar to the classical models provide a simple, interpretable estimation of demands with an improved fit to the entire responses. More particularly, using the clustering technique, this study investigates whether a single linear model is sufficient to capture the pattern in the response or the inherent volatility is statistically significant that necessitates generating different clusters and consequently separate demand models.

The remaining parts of the paper are organized as: in the first section, the applied methodology is described. Then, the procedures and detailing of the analytical modeling and seismic analysis of bridges are explained. In addition to the statistical visualization of data, the structure of the relationship between dynamic characteristics of considered bridges is illustrated in Section 3. Next, Section 4 provides a discussion of clustering data points for individual demands and then proposes a set of multi-level regression models to represent seismic demand models. Eventually, Section 5 summarizes the findings of this study.

2. Methodology

2.1. Regression Model for Seismic Demands

The demand models are typically expressed as a function of ground motion intensity as formulated in Equation (1).

$$S_D = aIM^b \quad (1)$$

In this equation, S_D denotes the median seismic demand of interest, and IM represents the considered intensity measure. The classical demand formulation presented in Equation (2) was initially introduced by Shome et al. (1998), and since then, it has been extensively applied (e.g., Gardoni, Mosalam, and Der Kiureghian 2003; Nielson 2005; Padgett and DesRoches 2007; Zhong et al. 2008) for the seismic assessment of various bridge types. For simplicity and based upon the lognormally distributed seismic demands (Cornell et al. 2002; Song and Ellingwood 1999), this relationship can be re-written in a linear regression format such that Equation (2).

$$\ln(S_D) = \ln(a) + b(\ln(IM)) \quad (2)$$

Based on this model, the logarithmic standard deviation or dispersion value is computed as

$$\beta_{D|IM} = \sqrt{\frac{\sum_{i=1}^n (\ln(p_i) - \ln(a) + b(\ln(IM)))^2}{n - 2}} \quad (3)$$

To efficiently represent the variation in the response, instead of developing a single PSDM (SPSDM) for each demand, multi-level probabilistic seismic demand models (MLPSDMs) are inspected in this study.

2.2. Identifying Clusters of Data Points

When the variability among data points is significant enough for individual seismic demands such as column curvature, separate clusters can be formed. To investigate this phenomenon, the k -means clustering algorithm is applied which leads to specify a set of clusters with similar bridge responses in each group. In this approach, clusters are defined by a central vector, and then, based on the number of clusters, the k cluster centers are defined. Next, the data points corresponding to the bridge responses are assigned to separate clusters based on their minimum squared distance from the centers. The breakdown of how this optimization problem is solved in an iterative process is as follows:

- Determine k number of clusters and randomly assign data points to the clusters;

$$\omega_{ij} = \begin{cases} 1 & \text{if data point } p_i \text{ belongs to cluster } j \\ 0 & \text{otherwise} \end{cases} \quad (4)$$

- Define the centroids ($c_j, j = 1, \dots, k$) of the pre-defined subgroups;
- Compute distance between all data points and the identified centroids;
- Minimize sum of squared distance (SSD) in the objective function displayed as:

$$F_{SSD} = \sum_{i=1}^n \sum_{j=1}^k \omega_{ij} \|p_i - c_j\|^2, \quad n = \text{total number of data points}; \quad (5)$$

- Next, assign data points to the closest subgroup based on their least distance to the clusters' centroid by assuming the centroids to be fixed and minimizing

$$\frac{\partial F_{SSD}}{\partial \omega_{ij}} = \sum_{i=1}^n \sum_{j=1}^k \|p_i - c_j\|^2; \quad (6)$$

- Then, the centroids need to be recomputed, as shown in Equation (7), to reflect the updated arrangement of the data points in each cluster.

$$\frac{\partial F_{SSD}}{\partial c_j} = 2 \sum_{i=1}^n \omega_{ij} (p_i - c_j) = 0 \Rightarrow c_j = \frac{\sum_{i=1}^n \omega_{ij} p_i}{\sum_{i=1}^n \omega_{ij}} \quad (7)$$

This statistical learning technique determines the optimal number of clusters by optimizing the Silhouette coefficients (SC), ranging from 0 to 1, that are representative of the degree of separation between the formed clusters. This metric is calculated for data point p_i as

$$SC_i = \begin{cases} 1 - \frac{\mu_{A_i}}{\mu_{B_i}} & \text{if } \mu_{A_i} < \mu_{B_i} \\ 0 & \text{if } \mu_{A_i} = \mu_{B_i} \\ \frac{\mu_{B_i}}{\mu_{A_i}} - 1 & \text{if } \mu_{A_i} > \mu_{B_i} \end{cases} \quad (8)$$

such that μ_{A_i} denotes the average distance of point p_i from all data points in the same cluster, and μ_{B_i} represents the average distance of point p_i from all data points in the closest cluster. The Silhouette value equal to zero indicates that a sample is located on the boundaries of two clusters, while the value equal to one represents a sample in a long distance to the neighboring clusters. However, a negative value means that the sample does not belong to the assigned cluster. In this study, each instance belongs to exactly one cluster so an overlap between the clusters is not considered.

Table 1. Description of the nomenclature assigned to the considered tall bridges.

Nomenclature	Bridge type	Abutment type	H_{ratio}	Type of analysis
MSTB-DLD	Multi-span tall bridge	Rigid diaphragm	Low	Deterministic
MSTB-DLP	Multi-span tall bridge	Rigid diaphragm	Low	Probabilistic
MSTB-SLD	Multi-span tall bridge	Seat	Low	Deterministic
MSTB-SLP	Multi-span tall bridge	Seat	Low	Probabilistic
MSTB-DMD	Multi-span tall bridge	Rigid diaphragm	Medium	Deterministic
MSTB-DMP	Multi-span tall bridge	Rigid diaphragm	Medium	Probabilistic
MSTB-SMD	Multi-span tall bridge	Seat	Medium	Deterministic
MSTB-SMP	Multi-span tall bridge	Seat	Medium	Probabilistic
MSTB-DHD	Multi-span tall bridge	Rigid diaphragm	High	Deterministic
MSTB-DHP	Multi-span tall bridge	Rigid diaphragm	High	Probabilistic
MSTB-SHD	Multi-span tall bridge </td <td>Seat</td> <td>High</td> <td>Deterministic</td>	Seat	High	Deterministic
MSTB-SHP	Multi-span tall bridge	Seat	High	Probabilistic

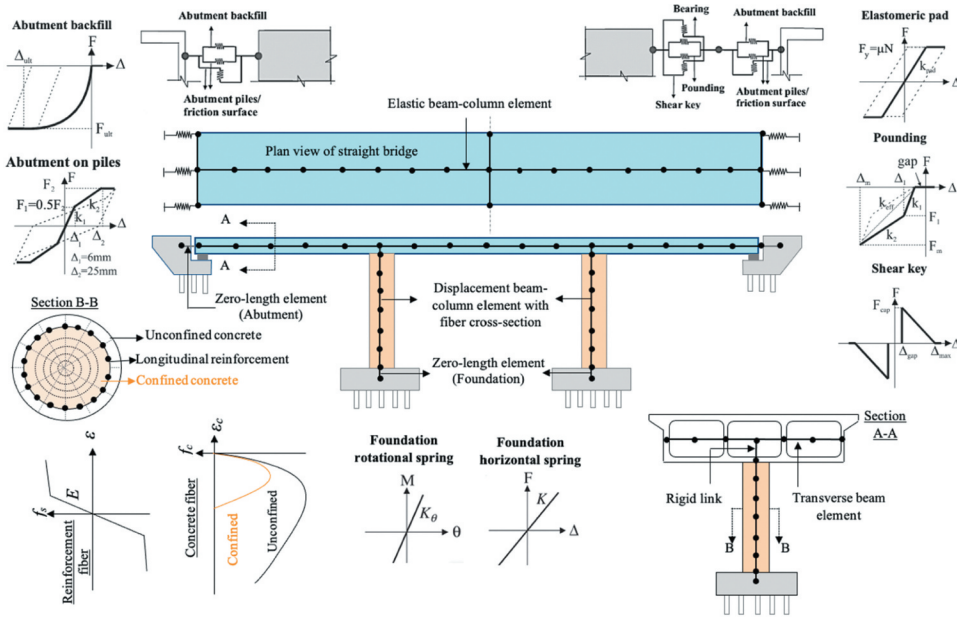


Figure 1. Schematic diagram for modeling a typical three-span box-girder concrete bridge.

3. Seismic Performance Analysis

To simplify the discussion of the results, nomenclatures, described in Table 1, are assigned to the considered bridges. Models for three-span and four-span bridges with the rigid diaphragm and seat type abutments are created in OpenSees (Mazzoni et al. 2007). The same procedure as explained in the work by Soleimani (2017), where a thorough description is found, is followed to construct bridge components. Then, the components are integrated to establish the bridge system, as demonstrated in the schematic diagram of Fig. 1. For the class of multi-span concrete box girder bridges that is considered in this study, characteristics of bridges constructed in California are adapted, and tall bridges are defined as those whose averaged column height is at least 1.5 times the averaged column height of a bridge with regular-sized columns (~7.5 m) (Mangalathu et al. 2018; Soleimani 2017). Three different ranges (i.e., Low, Medium, High) of column height ratios H_{ratio} , calculated as the average column height of tall piers divided by the average column height of normal piers, are used in the modeling of bridge piers. The values of H_{ratio} varies in the following spans: (1.5, 2.5), (2.5, 3.5), and (3.5, 4.5) for Low, Medium, and High ranges. Then, for individual bridges in Table 1, bridge samples

Table 2. Distribution of random variables used to create bridge models (Mangalathu Sivasubramanian Pillai 2017; Soleimani 2017).

	Parameter	Unit	Distribution	Distribution parameters	
				Factor 1*	Factor 2**
General	Concrete compressive strength	(Mpa)	Normal	34.5	
	Reinforcing steel yield strength	(Mpa)	Lognormal	6.14	4.3
	Mass factor	N/A	Uniform	1.1	2.0
	Damping	%	Normal	0.045	1.4 0.0125
Superstructure	Span length	(m)	Empirical	35.0	
	Deck width	(m)	Empirical	20.5	12.3
	Girder spacing	(cm)	Empirical	289.6	12.9
	Top flange thickness	(cm)	Empirical		100.1
	Reinforced concrete			21.3	
	Pre-stressed concrete			20.8	2.8
	Bottom flange thickness	(cm)	Uniform	11.4	2.5
	Wall thickness	(cm)	Uniform	25.4	16.5
	<u>Depth of superstructure</u>	(cm)	Uniform		30.5
	Reinforced concrete		Uniform	0.055* Span length	
	Pre-stressed concrete		Uniform	0.04* Span length	
	Substructure	<u>Column cross section dimension</u>	(cm)	Randomly assign equal portion of simulations to each	
Circular			152, 168, 183, 213, 274		
Rectangular			122x183, 122x244, 168x252, 183x274		
Longitudinal reinforcement ratio		N/A	Uniform	1.0	3.5
Confinement ratio		N/A	Uniform	0.4	1.7
Abutment backwall height		(m)	Uniform	1.1	2.6
Pile spacing		(m)	Uniform	1.7	2.1
Shear key capacity		(kN)	Normal	4884.2	646.8
Multiplicative factor for coefficient of friction of bearing pads		N/A	Lognormal	0	0.1
Shear modulus of elastomeric bearing pads		(Mpa)	Uniform	551.6	1723.9
Transverse gap between deck and shear keys		(mm)	Uniform	0	38.1
Longitudinal gap between deck and abutment		(mm)	Uniform	0	152.4
Pile stiffness		(kN/cm)	Lognormal	80.6	0.86
Foundation	<u>Foundation translational stiffness</u>	(kN/cm)	Normal		
	Single column – 6 ft dia column 1% long. steel			2977.2	1401.0
	Single column – 6 ft dia column 3% long. steel			2451.8	1050.8
	<u>Foundation rotational stiffness</u>	(kN-m/rad)	Normal		
	Single column – 6 ft dia column 1% long. steel			4632.4	1355.8
Single column – 6 ft dia column 3% long. steel			7344.0	1129.8	

*, ** Factors 1 and 2 are used to calculate the mean and standard deviation of normal, lognormal, and empirical distributions as well as the lower and upper bounds of uniform distribution

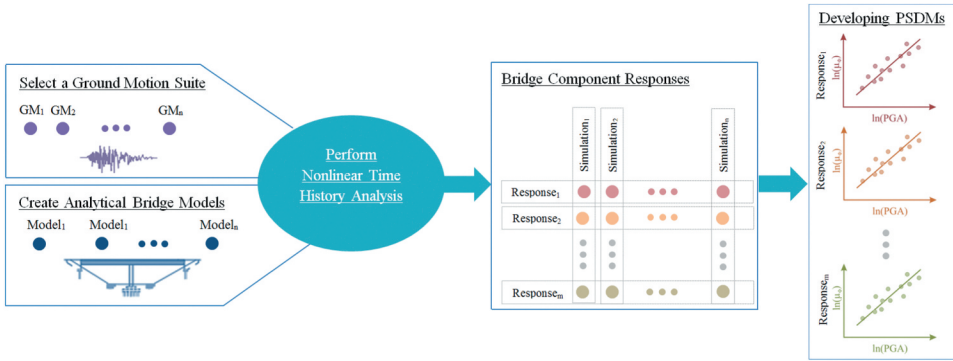


Figure 2. Illustrative procedure for developing probabilistic seismic demand model of a bridge.

are formed by randomly picking values from the probability distribution of the modeling parameters (mean and standard deviation of the fitted distributions are provided in Table 2) following the Latin Hypercube technique (Ayyub and Lai, 1989).

The distribution of modeling parameters that is used in this study was extracted from the existing bridge inventory in California. For a detailed explanation of the data and distribution derivation of each parameter, interested readers are encouraged to refer to the previous comprehensive reports (Mangalathu Sivasubramanian Pillai 2017; Soleimani 2017). The current study conducts two types of analysis, as mentioned in Table 1. Although in the probabilistic assessment of bridges, the values of structural modeling parameters are randomly selected from the distribution of variables provided in Table 2, the median values are chosen for each modeling parameter in the deterministic evaluation. The bridge samples are randomly paired with the selected ground motions. Through Nonlinear Time History Analysis (NLTHA), bridge seismic responses are estimated, and their peak values are recorded at the longitudinal and orthogonal components of the Baker’s suite (Baker et al. 2011) of ground motion excitations. The general procedure of developing PSDMs is demonstrated in Fig. 2. The recorded seismic demand parameters include column curvature ductility D_{Col} , deck displacement D_{Deck} , translational and rotational movement of the foundation $D_{Fnd_{trn}}$ and $D_{Fnd_{rot}}$, active, passive, and transverse displacements of the abutment $D_{Abut_{act}}$, $D_{Abut_{pass}}$, and $D_{Abut_{trn}}$, respectively.

4. Descriptive Statistical Analysis

4.1. Basic Statistics Data Visualization

First, the bivariate correlation among the extracted data is visualized. A matrix of the scatter plots of the demands (zero mean normalized), as presented by Fig. 3, discloses the correlation among the demand parameters. Among the seven monitored bridge responses, the active and passive displacements of the abutment and also the deck displacement, and transverse deformation of the abutment are found to be strongly and positively correlated with each other. However, other parameters display a weak, positive correlation with one another, such as the column curvature ductility and the transverse movement of the foundation. Interestingly, the foundation translational and rotational displacements are observed to be moderately correlated. Besides, the distribution of the demands along the diagonal cells of the matrix represents a histogram of the data according to the log-normal distribution of the bridge seismic responses.

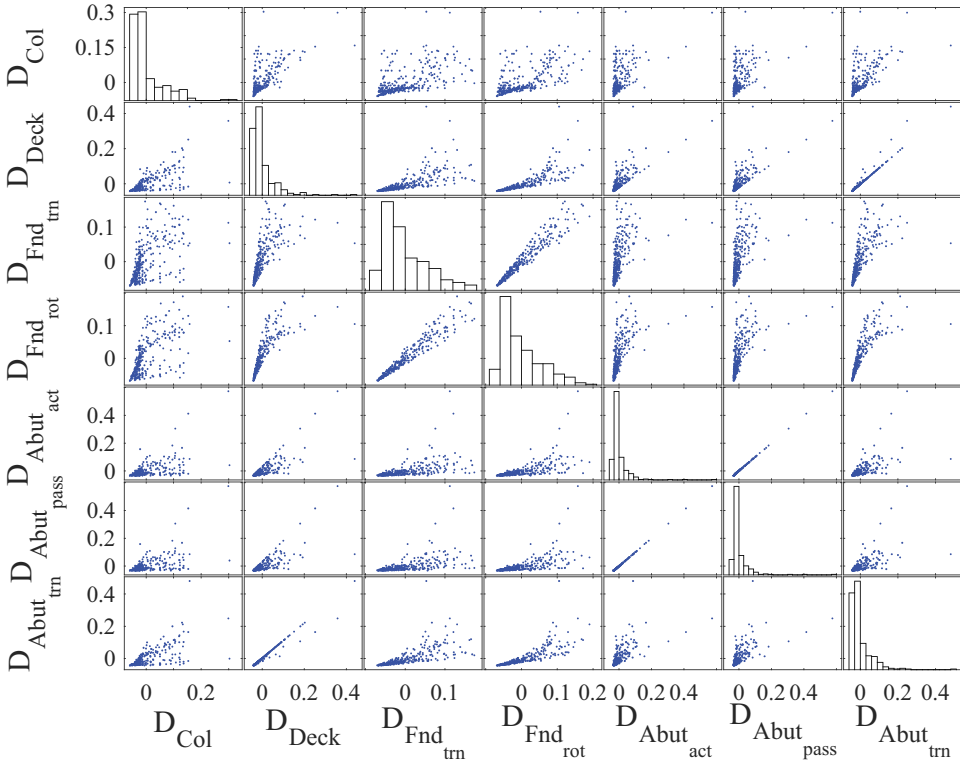


Figure 3. Correlation and distribution plot of the demand parameters for MSTB-DLD.

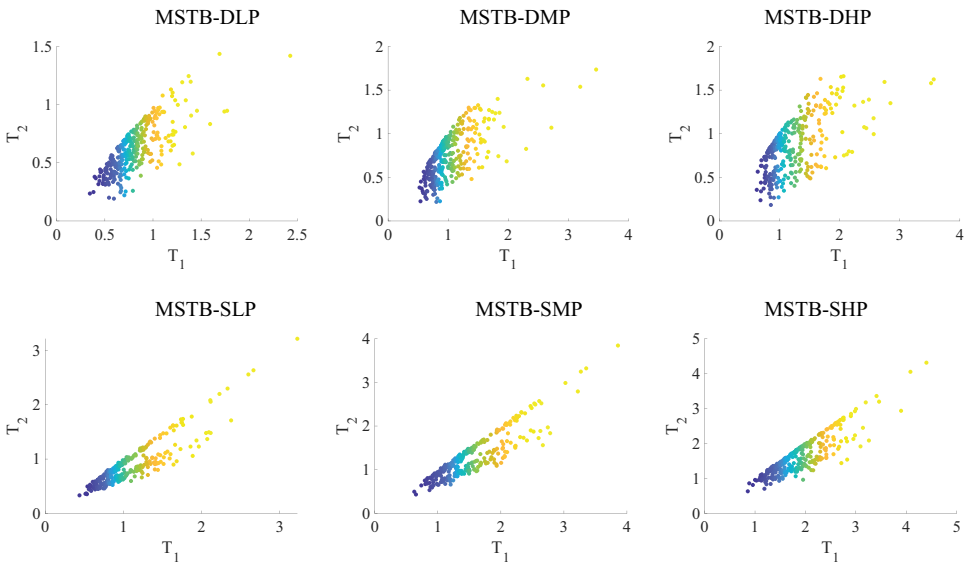


Figure 4. Relationship between the dynamic characteristics of analyzed bridges.

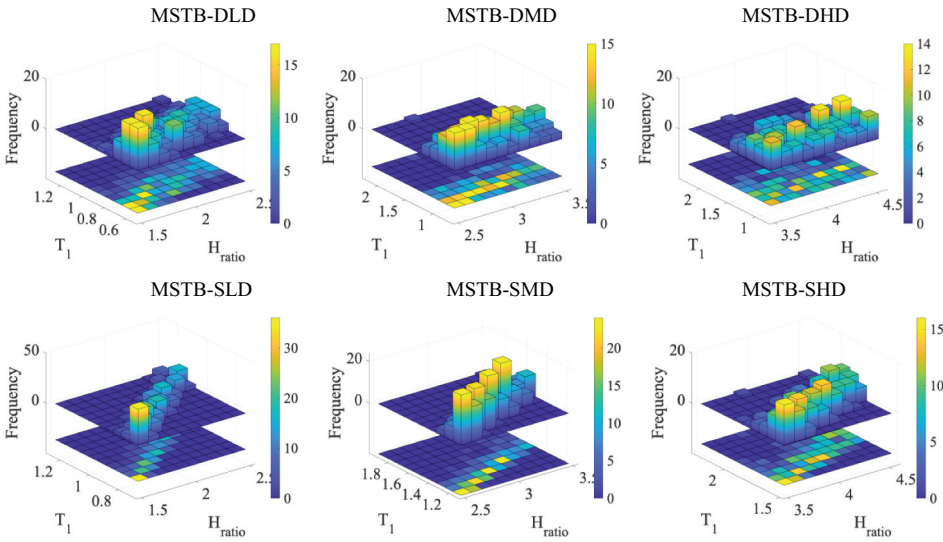


Figure 5. Variation of fundamental periods with respect to the changes in the pier height.

4.2. The Correlation between Dynamic Characteristics of Bridges

The natural frequencies as the underlying dynamic properties of the bridges are investigated through a multi-degree structure eigenvalue analysis. The correlation between the first (T_1) and second (T_2) fundamental vibration periods of bridges are presented in Fig. 4.

The generally observed trend in almost all plots is that T_1 and T_2 changes are in the same direction showing a positive correlation. If the column height is changed from low to high, the natural frequencies change to be more scattered but the direct relationship between T_1 and T_2 remains unaffected. This implies that the variability in the seismic responses is higher in irregular bridges compared to normal bridges and increases as the column height increase. In the probabilistic cases, the fundamental periods are more closely correlated compared to the deterministic scenarios. In bridges with seat type abutment, T_1 and T_2 are tightly related, and in the probabilistic cases, the pattern shows a more well-defined correlation compared to the deterministic ones.

Furthermore, the sensitivity of the fundamental periods of bridges is explored with respect to the column height ratios (Fig. 5). An increasing trend is observed in the relation of fundamental periods to the column height ratios. This trend is more visible in the results of the deterministic analysis and particularly noticeable for bridges with seat abutments. It is discovered that the dynamic properties of tall bridges with seat abutments are more sensitive to the column height ratios. A more well-defined linear relationship is observed between T_1 and H_ratio in the lower range of column heights (e.g. MSTB-DLD vs MSTB-DHD) which is due to the increased variability in the seismic demands in bridges with higher ranges of column heights. Because of the aforementioned positive correlation between T_1 and T_2 , similar patterns are observed for the T_2 - H_ratio data sets.

5. Diagnostic Statistical Analysis and Multi-level Regression Models

In order to derive probabilistic seismic demand models, the engineering demand parameters captured during the seismic analyses of bridges are plotted (Figs. 6–9) against the intensity measures of the applied ground motions, after transforming both to the logarithmic space. In Figs. 6–9 the points are color-coded to visibly differentiate formed clusters or subgroups. The numbers assigned to the subgroups of data are displayed in the legends.

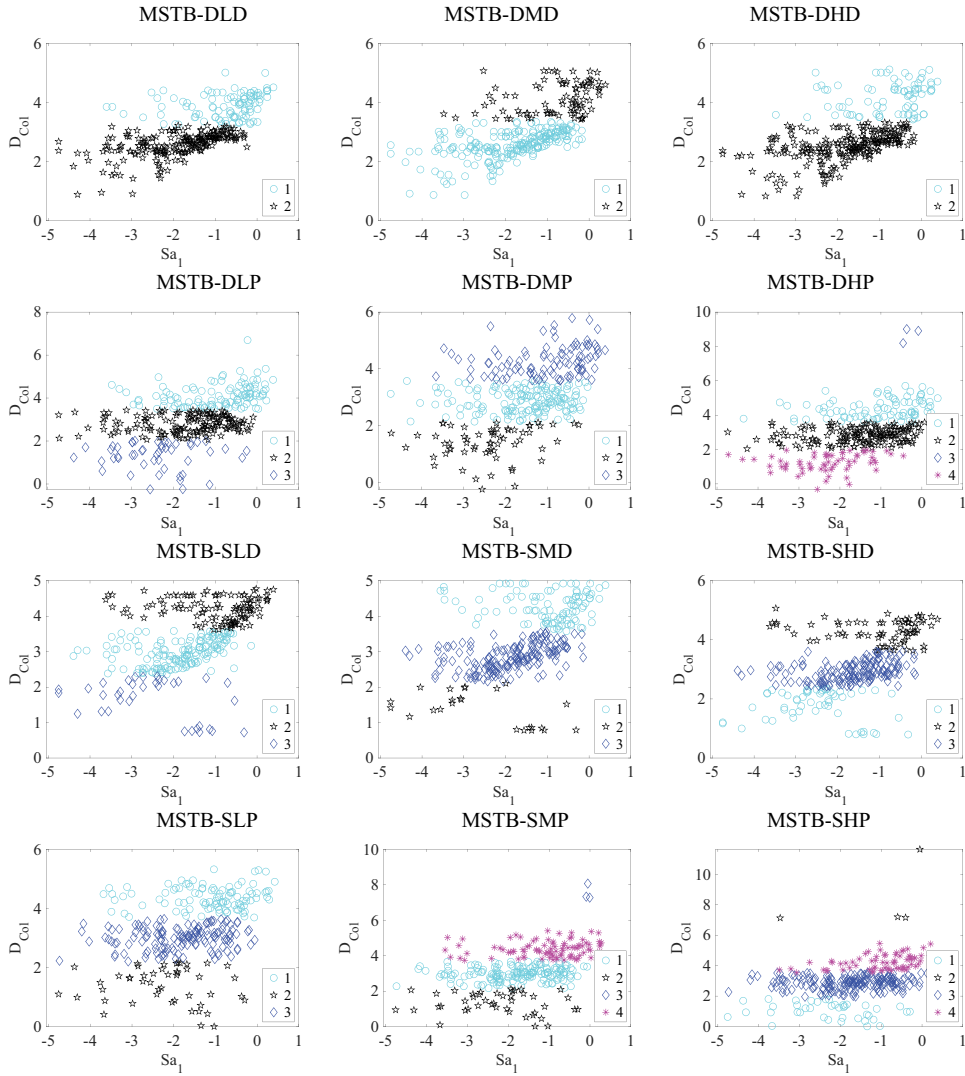


Figure 6. Probabilistic seismic demands (in logarithmic scale) for the column curvature ductility (the numbers in the legend represent cluster numbers).

It is observed that the plots with more scattered data points consist of more distinct groups as a result of increased variation in the responses. For instance, the points corresponding to the column curvature ductility of deterministic analysis of rigid diaphragm bridges (the first row in Fig. 6) form two clusters, one in cyan and another in black. For example, for MSTB-DLD, the cyan cluster tends to be higher in demand values than the black one which means this clustering algorithm is dominated by the demand values independent of the intensity measure. A similar clustering trend is observed in the other plots of the demands corresponding to the column and the abutment and obtained from the analysis of the other bridge types (Figs. 6 and 9). However, in the case of deck displacement and the movement of the foundation belonging to the bridges with rigid diaphragm abutments, as displayed in Figs. 7 and 8, the cluster formation depends on both values of demand and excitation intensity. In these cases, demands typically increase with a monotonic trend as the ground motions get stronger.

A similar procedure is followed for other types of bridges to check the possibility of dividing the population of demands data into a number of groups based on their similar pattern. The demand patterns, clustering design, and the optimal group numbers are found to be almost the same for the

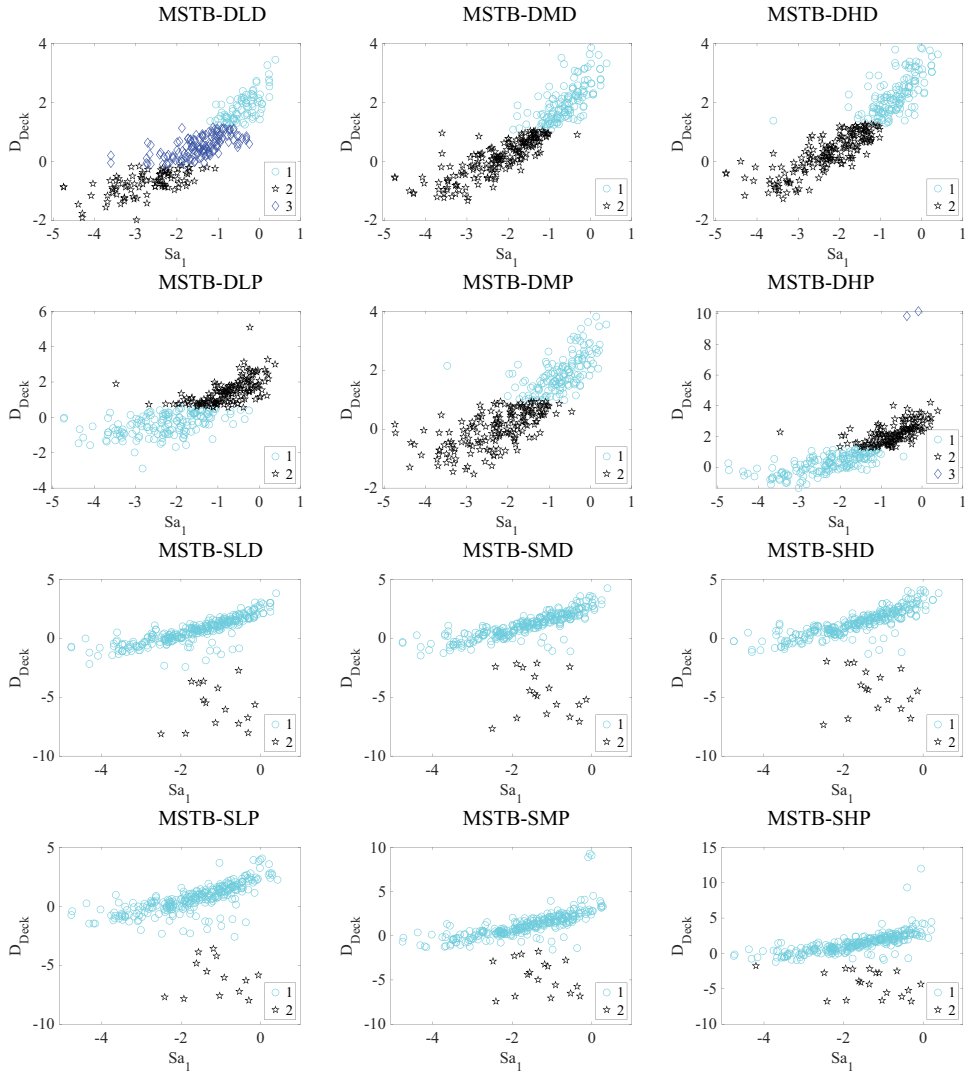


Figure 7. Probabilistic seismic demands (in logarithmic scale) for the deck displacement (the numbers in the legend represent cluster numbers).

highly correlated responses. Depending on the bridge type and the analyzed seismic demand, a various number of clusters are distinguished and summarized in [Table 3](#).

Evaluating specific demands, the optimum number of clusters is diverse for the column curvature ductility, changing from two to four. However, the deck and foundation demands are mostly partitioned into two groups by a couple of exceptions. Regarding the related demands to the abutment, although the majority of them are represented by three distinct clusters, many are divided by two clustered. Assessing particular bridge types, two or three group numbers are optimized for demands of almost all bridge types, while $\sim 35\%$ of the results related to the probabilistic analysis of bridges with seat abutments consist of four groupings. In general, two clusters occupy the majority of groupings in bridges with rigid diaphragm abutment that shows less variation in the seismic response of this type of bridge compared to the bridges consisting of seat abutments.

The highest population of groupings belongs to two clusters, as illustrated in all plots provided in [Fig. 10](#), which concisely overviews highlights of this section. Three is the next most common

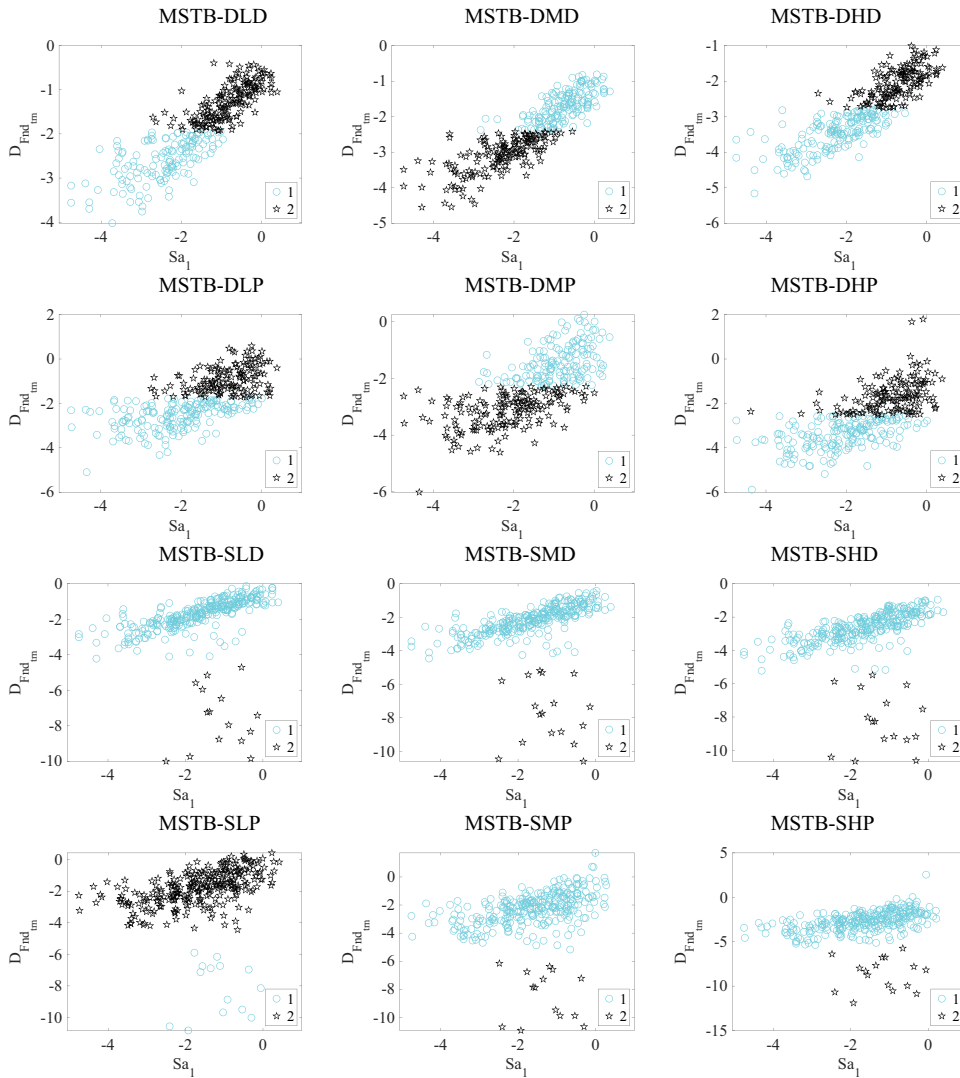


Figure 8. Probabilistic seismic demands (in logarithmic scale) for the translational movement of the foundation (the numbers in the legend represent cluster numbers).

clustering, and four and five are the rarest separations. An increase in the variation of the seismic demands is observed as the pier height ratio increases. Comparing the frequency of produced subgroups between different ranges of pier height ratios reveals that the responses corresponding to the low column heights tend toward a lower (i.e. either 2 or 3) number of clusters. However, the demands of bridges with medium and high heights could have 2, 3, and 4 subgroups with the highest frequency related to two clusters. Besides, the evaluation of grouping counts among varied abutment types affirms that more dissimilarities are detected in the response of bridges with seat abutments than the ones with the rigid type.

Further, the assessment of the number of formed subgroups within different types of analysis exhibit equal allocations of two numbers of clustering. The results obtained from the deterministic analysis are either formed as two or three clusters, though the results gained from the probabilistic analysis are distributed throughout multiple groupings due to the higher level of response variation in the latter one caused by the associated uncertainties involved in the procedure. Moreover, according to

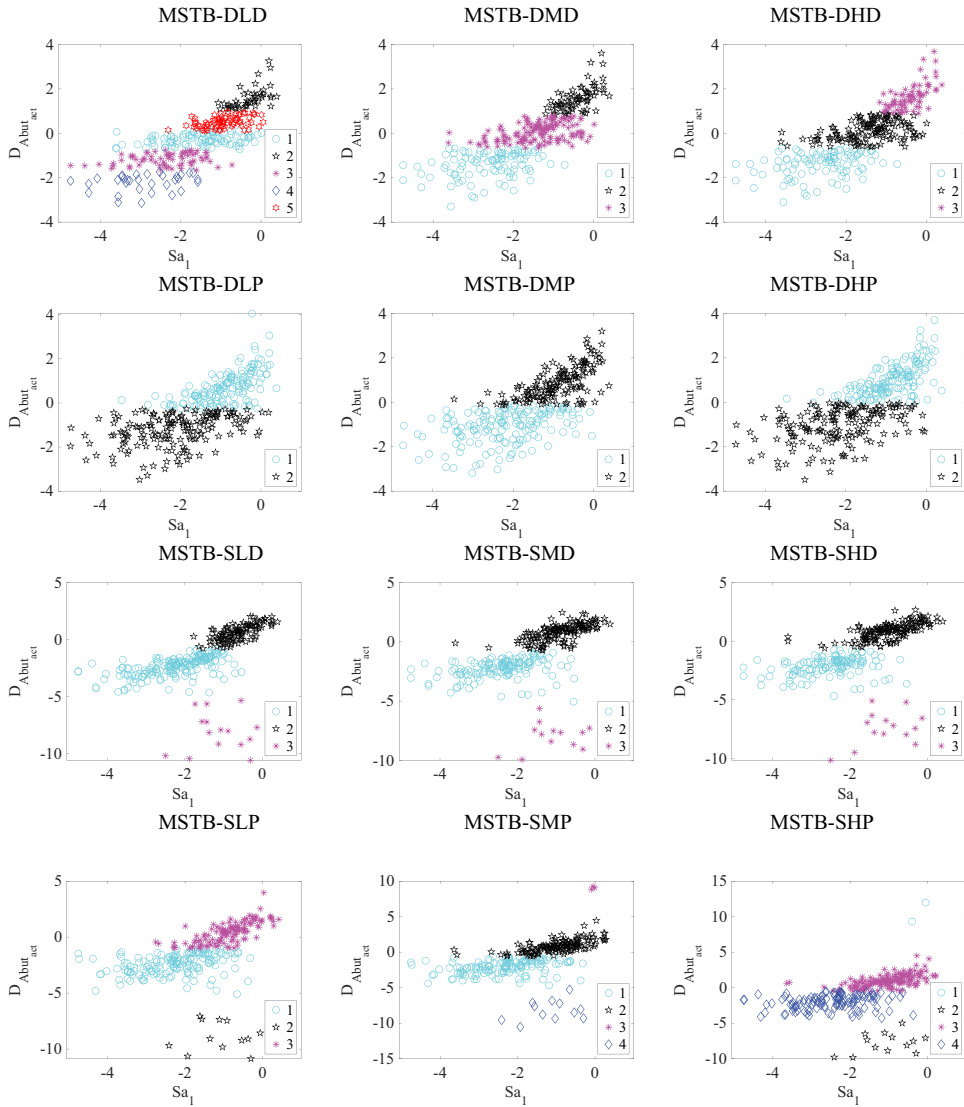


Figure 9. Probabilistic seismic demands (in logarithmic scale) for the active displacements related to the abutment (the numbers in the legend represent cluster numbers).

the overall distribution comparison of these quantities among diverse seismic demands, although column responses can be divided into 2, 3, or 4 clusters, they are more prone to have three groupings, similar to the active and passive responses of the abutments. The graphical distribution declares that the deck and foundation demands are mostly assigned to two clusters due to their more uniform results compared to the other bridge components.

Based on the presented results in the previous section, noticeable dissimilarity in the demand values leads to partition data into distinctive clusters. Two and three are found to be the common optimum choices as the grouping numbers; however, in scenarios with larger inconsistencies, four and five clusters of data points are formed. A separate univariate regression model is generated and examined for each distinguished cluster. [Figure 11](#) illustrates examples of the developed models, on a logarithmic scale, to clarify the concepts of generating MLPSDMs. Likewise, [Fig. 12](#) provides the mean squared errors (MSE) that ascertain better fitness of MLPSDMs compared to the single PSDMs. In order to provide an

Table 3. Summary of the number of clusters identified for various demands and bridge types.

Seismic demand	Nomenclature											
	MSTB-DLD	MSTB-DMD	MSTB-DHD	MSTB-DLP	MSTB-DMP	MSTB-DHP	MSTB-SLD	MSTB-SMD	MSTB-SHD	MSTB-SLP	MSTB-SMP	MSTB-SHP
D _{col}	2	2	2	3	3	4	3	3	3	3	4	4
D _{Deck}	3	2	2	2	2	3	2	2	2	2	2	2
D _{Fnd_trn}	2	2	2	2	2	2	2	2	2	2	2	2
D _{Fnd_rot}	2	2	2	5	2	3	2	2	2	2	2	2
D _{Abut_act}	3	3	3	2	2	2	3	3	3	3	4	4
D _{Abut_pass}	3	3	2	2	2	2	3	3	3	3	3	4
D _{Abut_trn}	3	2	2	2	2	3	3	2	2	3	2	2

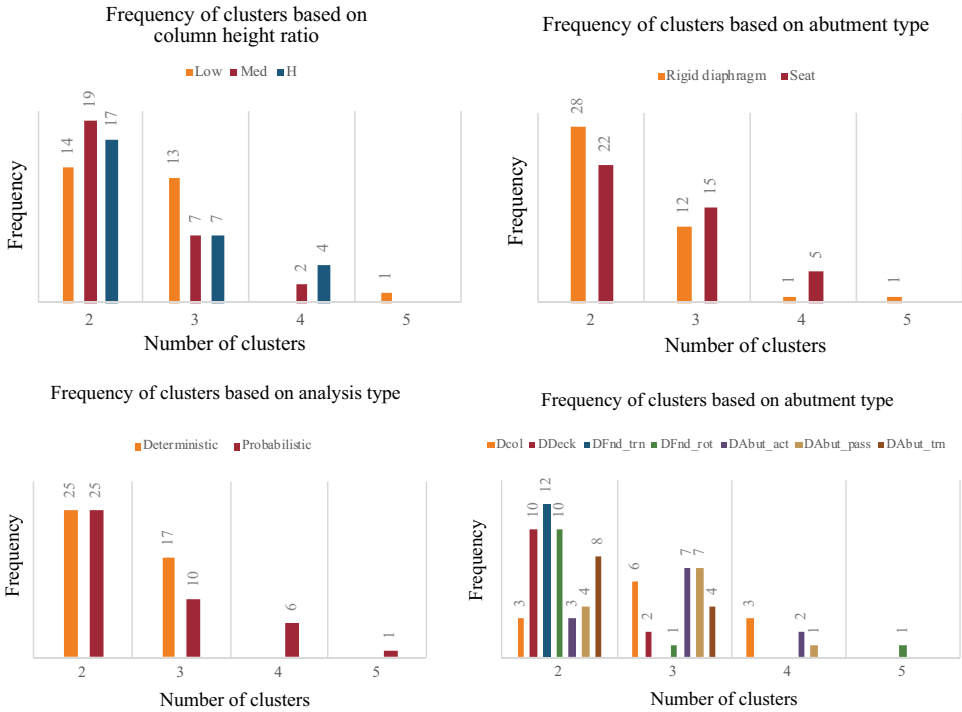


Figure 10. Comparison of the number of subgroups based on the variations in the column height ratios, model of abutment, type of analysis, and kind of demands.

unbiased statistical comparison, the MSE values of MLPSDMs and the associated clustered data points are integrated to report a single error value. By combining MSEs, the performance of developed SPSDMs and MLPSDMs are comparable for the entire and equal number of data points corresponding to each seismic demand. According to the results, the MSE values indicate higher variance in the responses according to the analysis of bridges with seat abutments than those of the bridges with rigid diaphragms.

Table 4 for bridges with rigid diaphragm and Table 5 for bridges with seat abutments compare developing a single PSDM, represented as M_0 , versus MLPSDM, listed as M_i where $i = 1, 2, \dots, 5$. In order to validate the results from clustering analyses, these comparisons are performed using analysis of covariance to express if the statistical difference between generated regression models is significant. The provided p -values are calculated through multiple comparison tests of the hypothesis that either the slopes or intercepts of the developed models are the same. Based on the considered 0.05 cut-off value, small p -values in *Italic* in Tables 4 and 5, prove the hypothesis. This justifies that with 95%

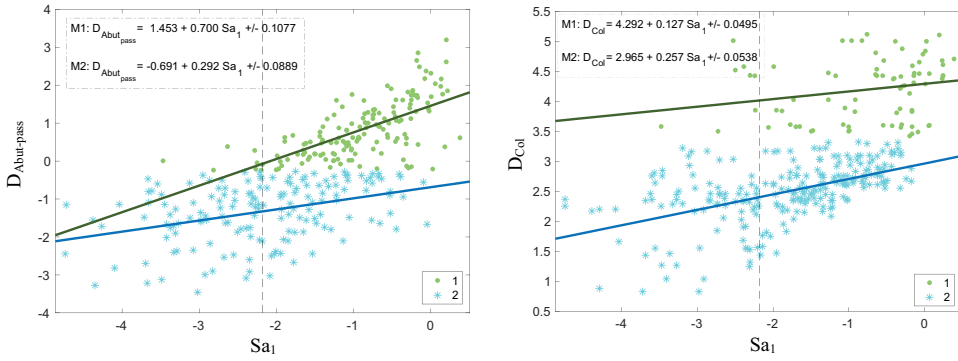


Figure 11. Multi-level probabilistic seismic demand models corresponding to the: (left) passive abutment responses of MSTB-DHD; (right) column responses of MSTB-DMP.

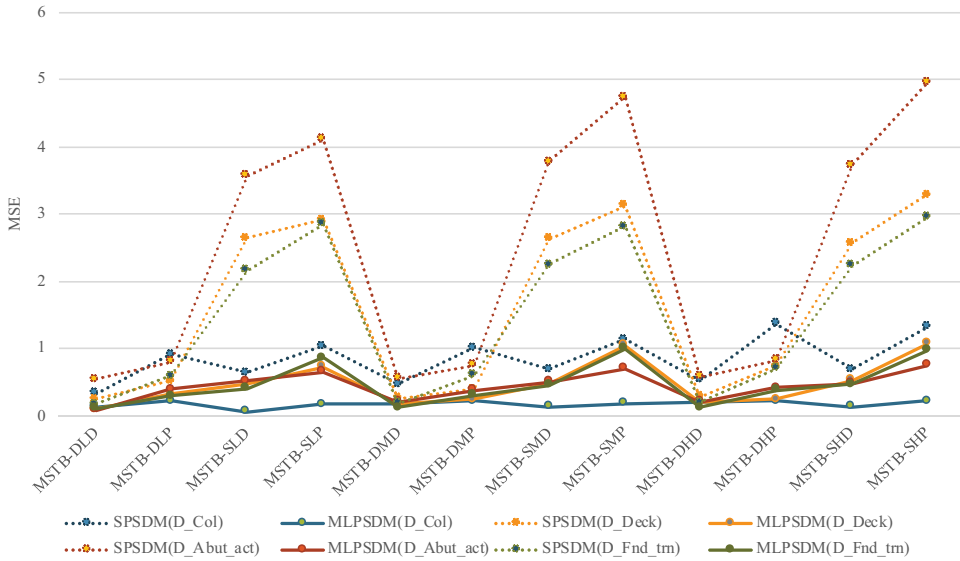


Figure 12. Comparison of the mean squared errors of the developed models.

confidence the discrepancies in the identified clusters resulted from the analyses of the previous section are noticeable to assign MLPSDMs in an individual seismic demand of a bridge.

On the other side, the large p -values reject the hypothesis meaning that, in those cases, creating separate models for each cluster is not a reasonable approach. In most cases, the reported p -values corresponding to the slope (a) and the intercept (b) indicate that one or the other value is under the cut-off point. Therefore, the statistical comparison results presented in this section affirm that multiple models are required to present the unique seismic performance of tall bridges, and the groupings optimized by the clustering algorithm can set up the basis to establish the best choice for generating MLPSDMs. However, there are a few exceptions, all belong to the bridge with rigid diaphragm abutment, among the reported p -values (bold values in Table 4) where it is seen that neither the slope value related to the slope nor the one belongs to the intercept are small enough to prove the concept. Interestingly, one of those cases belongs to the rotational movement of the foundation for MSTB-DLP in which five clusters were designed. This was the only case with the five clusters; however, this is not validated based on the comparison of the generated regression models, thus four groupings would be sufficient in this case.

Table 4. Comparison of the developed MLPSDMs for bridges with rigid diaphragm abutment.

Bridge Type	PSDMs	p-values													
		D _{col}		D _{Dec}		D _{Fnd_trn}		D _{Fnd_rot}		D _{Abut_act}		D _{Abut_pass}		D _{Abut_trn}	
		a	b	a	b	a	b	a	b	a	b	a	b	a	b
MSTB-DLD	M0	0.00	0.00	0.00	0.00	0.00	0.00	0.00	0.00	0.01	0.00	0.11	0.00	0.00	0.00
	M1	0.00	0.01	0.00	0.00	0.00	0.02	0.00	0.01	0.00	0.00	0.46	0.00	0.07	0.00
	M2	0.00	0.01	0.00	0.00	0.00	0.02	0.00	0.01	0.00	0.01	0.00	0.00	0.00	0.00
	M3	-	-	0.19	0.00	-	-	-	-	0.00	0.00	0.00	0.00	0.00	0.00
	M4	-	-	-	-	-	-	-	-	0.00	0.58	-	-	-	-
MSTB-DLP	M0	0.00	0.13	0.00	0.00	0.00	0.00	0.00	0.00	0.00	0.00	0.01	0.00	0.00	0.00
	M1	0.00	0.03	0.00	0.00	0.00	0.59	0.91	0.16	0.00	0.00	0.00	0.00	0.00	0.00
	M2	0.44	0.61	0.00	0.00	0.00	0.59	0.00	0.01	0.00	0.00	0.00	0.00	0.00	0.00
	M3	0.00	0.16	-	-	-	-	0.00	0.13	-	-	-	-	-	-
	M4	-	-	-	-	-	-	0.00	0.41	-	-	-	-	-	-
MSTB-DMD	M0	0.00	0.00	0.00	0.00	0.00	0.00	0.00	0.00	0.00	0.00	0.00	0.00	0.00	0.00
	M1	0.00	0.21	0.00	0.00	0.00	0.10	0.00	0.02	0.00	0.00	0.00	0.00	0.00	0.00
	M2	0.00	0.21	0.00	0.00	0.00	0.10	0.00	0.02	0.00	0.00	0.00	0.00	0.00	0.00
	M3	-	-	-	-	-	-	-	-	0.17	0.00	0.34	0.00	-	-
	M4	-	-	-	-	-	-	0.00	0.88	-	-	-	-	-	-
MSTB-DMP	M0	0.00	0.00	0.00	0.00	0.00	0.00	0.00	0.00	0.00	0.00	0.00	0.00	0.00	0.00
	M1	0.00	0.18	0.00	0.03	0.00	0.23	0.00	0.86	0.00	0.00	0.00	0.00	0.00	0.14
	M2	0.00	0.73	0.00	0.03	0.00	0.23	0.00	0.86	0.00	0.00	0.00	0.00	0.00	0.14
	M3	0.23	0.05	-	-	-	-	-	-	-	-	-	-	-	-
	M4	0.00	0.00	0.00	0.00	0.00	0.00	0.00	0.00	0.00	0.00	0.00	0.00	0.00	0.00
MSTB-DHD	M0	0.00	0.05	0.00	0.04	0.00	0.25	0.00	0.02	0.00	0.00	0.00	0.00	0.00	0.05
	M1	0.00	0.05	0.00	0.04	0.00	0.25	0.00	0.02	0.00	0.00	0.00	0.00	0.00	0.05
	M2	0.00	0.05	0.00	0.04	0.00	0.25	0.00	0.02	0.00	0.00	0.00	0.00	0.00	0.05
	M3	-	-	-	-	-	-	-	-	0.26	0.00	-	-	-	-
	M4	0.00	0.31	0.00	0.35	0.00	0.00	0.00	0.00	0.00	0.00	0.00	0.00	0.00	0.36
MSTB-DHP	M0	0.85	0.52	0.00	0.93	0.00	0.28	0.00	0.24	0.00	0.00	0.00	0.00	0.00	0.78
	M1	0.00	0.46	0.00	0.75	0.00	0.28	0.00	0.00	0.00	0.00	0.00	0.00	0.00	0.84
	M2	0.00	0.40	0.00	0.84	-	-	0.07	0.01	-	-	-	-	0.00	0.90
	M3	0.00	0.46	-	-	-	-	-	-	-	-	-	-	-	-
	M4	0.00	0.46	-	-	-	-	-	-	-	-	-	-	-	-

6. Discussions

Important findings from this study are highlighted in the following remarks. As denoted in the results, the common assumption of a single linear fit between the seismic demand and ground motion intensity is not compatible with all bridge types and particularly bridges with irregular configurations. This is mainly due to the distinct seismic performance of bridges with geometric irregularities. More specifically, this study indicates that the classical single linear regression model is not able to thoroughly capture the significant variability that is observed in the seismic demands of tall bridges.

Based on the analysis results of the concrete box-girder bridges, the existing variability induces the formation of clusters of data. The identified clusters necessitate developing individual demands models for each. According to the results, MLPSDMs provide a more reliable estimation of the seismic demands compared to the SPSMDs.

The MLPSDMs provide a fruitful insight regarding the seismic performance of various components of a bridge. In order to use MLPSDMs to produce fragility curves, conditional MLPSDMs can be considered to set conditions for the demand and ground motion intensity values to switch between different models based on the defined ranges. Another alternative, for the application to the fragility analysis of bridges, is using piecewise linear regression models which can yet represent the formation of clusters in demands. The proposed approach in this study still follows the linear relationship between the demands and intensities. However, by defining clusters, the variability in the demands is efficiently captured.

Table 5. Comparison of the developed MLPSDMs for bridges with seat abutment.

Bridge Type	PSDMs	p-values													
		D _{col}		D _{Dec}		D _{Fnd_trn}		D _{Fnd_rot}		D _{Abut_act}		D _{Abut_pass}		D _{Abut_trn}	
		a	b	a	b	a	b	a	b	a	b	a	b	a	b
MSTB-SLD	M0	0.00	0.49	0.00	0.00	0.00	0.01	0.00	0.19	0.00	0.00	0.00	0.00	0.00	0.00
	M1	0.00	0.62	0.00	0.01	0.00	0.06	0.00	0.00	0.00	0.01	0.00	0.00	0.00	0.00
	M2	0.00	0.00	0.00	0.01	0.00	0.06	0.00	0.00	0.00	0.87	0.00	0.02	0.00	0.04
	M3	0.00	0.00	-	-	-	-	-	-	0.00	0.00	0.00	0.99	0.00	0.11
MSTB-SLP	M0	0.00	0.69	0.00	0.05	0.00	0.09	0.00	0.53	0.00	0.00	0.00	0.00	0.00	0.01
	M1	0.01	0.15	0.00	0.01	0.00	0.24	0.00	0.00	0.00	0.00	0.00	0.00	0.01	0.05
	M2	0.00	0.59	0.00	0.01	0.00	0.24	0.00	0.00	0.00	0.03	0.00	0.41	0.00	0.00
	M3	0.00	0.12	-	-	-	-	-	-	0.00	0.33	0.00	0.04	0.00	0.22
MSTB-SMD	M0	0.00	0.34	0.00	0.32	0.00	0.34	0.00	0.18	0.00	0.00	0.00	0.00	0.00	0.68
	M1	0.00	0.47	0.00	0.00	0.00	0.00	0.00	0.00	0.00	0.08	0.00	0.05	0.00	0.00
	M2	0.00	0.00	0.00	0.00	0.00	0.00	0.00	0.00	0.00	0.74	0.00	0.80	0.00	0.00
	M3	0.00	0.00	-	-	-	-	-	-	0.00	0.02	0.00	0.10	-	-
MSTB-SMP	M0	0.00	0.87	0.00	0.43	0.00	0.62	0.00	0.32	0.04	0.77	0.00	0.00	0.00	0.89
	M1	0.00	0.84	0.00	0.00	0.00	0.02	0.00	0.00	0.00	0.94	0.00	0.03	0.00	0.00
	M2	0.00	0.89	0.00	0.00	0.00	0.02	0.00	0.00	0.00	0.94	0.00	0.41	0.00	0.00
	M3	0.00	0.86	-	-	-	-	-	-	0.00	0.91	0.00	0.48	-	-
	M4	0.00	0.85	-	-	-	-	-	-	0.00	0.84	-	-	-	-
MSTB-SHD	M0	0.00	0.80	0.00	0.12	0.00	0.17	0.00	0.34	0.00	0.00	0.00	0.00	0.00	0.49
	M1	0.00	0.05	0.00	0.00	0.00	0.00	0.00	0.00	0.00	0.00	0.00	0.01	0.00	0.00
	M2	0.00	0.24	0.00	0.00	0.00	0.00	0.00	0.00	0.00	0.47	0.00	0.18	0.00	0.00
	M3	0.04	0.00	-	-	-	-	-	-	0.00	0.23	0.00	0.74	-	-
MSTB-SHP	M0	0.00	0.95	0.00	0.12	0.00	0.09	0.00	0.34	0.00	0.00	0.00	0.00	0.00	0.49
	M1	0.01	0.00	0.00	0.00	0.00	0.00	0.00	0.00	0.00	0.23	0.00	0.74	0.00	0.00
	M2	0.00	0.43	0.00	0.00	0.00	0.00	0.00	0.00	0.00	0.47	0.00	0.18	0.00	0.00
	M3	0.00	0.01	-	-	-	-	-	-	0.00	0.00	0.00	0.01	-	-

7. Conclusions

As an essential step towards the risk assessment of bridges, this study aimed to enhance understanding of the seismic performance of bridges with tall piers since this area has not been explored thoroughly yet. For this purpose, nonlinear time history analysis was carried out on tall concrete bridges. The statistical correlation between the seismic responses in addition to the exploratory data analysis including clustering analyses was conducted on the seismic demands. To explore intuition about the structure of seismic responses, the implemented clustering algorithm disclosed intrinsic grouping among collected data on the basis of similarity and dissimilarity between them. The groupings optimized by the clustering algorithm can set up the basis to establish the best choice for generating MLPSDMs. Depending on the identified optimum number of clusters, multiple linear regression models were generated and tested for individual demands.

In general, two clusters occupied the majority of groupings in the seismic responses of bridges with rigid diaphragm abutment that implies less variation in the seismic response of this type of bridge compared to the bridges consisting of seat abutments. An increase in the variation of the seismic demands was observed as the pier height ratio increases. Since, in most cases, the demands were categorized into two clusters, two separate linear models would be sufficient to capture the variability in the response. The results obtained from the deterministic analysis were either formed as two or three clusters, though the results gained from the probabilistic analysis were distributed throughout multiple groupings due to the higher level of response variation in the latter one caused by the associated uncertainties involved in the procedure. Therefore, the nonlinearity in the relationship between the demands and the ground motion intensity is more critical in the probabilistic analysis compared to the deterministic evaluation.

Overall, unique characteristics were detected in the seismic performance of considered bridges, and noticeable variations were observed in the seismic demands. The evaluation results implicated better performance of cluster-wise multiple models than a single model to represent the variation in the

bridge demands. Contrary to the bridges with ordinary piers in which single PSDMs are capable to properly represent the seismic demands, this study recommended developing multi-level PSDMs for bridges with tall piers to efficiently represent the variation in the response. Hence, a set of multi-level cluster-wise PSDMs were derived, and the optimal number of models were statistically tested. Further studies are required to focus on exploring the nonlinearity in the PSDMs and propose appropriate solutions. Besides, the findings of this study are limited to the concrete box-girder bridges. Further research is needed to investigate the performance of other types of bridges, such as T-girder and I-girder, with tall piers compared to normal bridges.

ORCID

Farahnaz Soleimani  <http://orcid.org/0000-0001-7809-2978>

References

- Abdel-Mohti, A., and G. Pekcan. 2008. Seismic response of skewed RC box-girder bridges. *Earthquake Engineering and Engineering Vibration* 7 (4): 415–26. doi: [10.1007/s11803-008-1007-4](https://doi.org/10.1007/s11803-008-1007-4).
- Ayyub, B. M., and K. L. Lai. 1989. Structural reliability assessment using Latin hypercube sampling. In *Proc., 5th Int. Conf. on Struct. Safety and Reliability, ICOSSAR'89*, Vol. 2, 1177–1184. New York: ASCE.
- Baker, J. W., T. Lin, S. K. Shahi, and N. Jayaram. 2011. New ground motion selection procedures and selected motions for the PEER transportation research program. *PEER Report* 3.
- Buckle, I., 1994. The Northridge, California earthquake of January 11, 1994: Performance of highway bridges. Tech. Rep. NCEER-94-0068, National Center for Earthquake Engineering Research.
- Button, M. R., C. J. Cronin, and R. L. Mayes. 2002. Effect of vertical motions on seismic response of highway bridges. *Journal of Structural Engineering* 128 (12): 1551–64. doi: [10.1061/\(ASCE\)0733-9445\(2002\)128:12\(1551\)](https://doi.org/10.1061/(ASCE)0733-9445(2002)128:12(1551)).
- Chen, X. 2020. System fragility assessment of tall-pier bridges subjected to near-fault ground motions. *Journal of Bridge Engineering* 25 (3): 04019143. doi: [10.1061/\(ASCE\)BE.1943-5592.0001526](https://doi.org/10.1061/(ASCE)BE.1943-5592.0001526).
- Chen, X., N. Xiang, J. Li, and Z. Guan. 2020. Influence of near-fault pulse-like motion characteristics on seismic performance of tall pier bridges with fragility analysis. *Journal of Earthquake Engineering*, 1–22. doi:10.1080/13632469.2020.1751345
- Chen, X., Z. Guan, J. Li, and B. F. Spencer Jr. 2018. Shake table tests of tall-pier bridges to evaluate seismic performance. *Journal of Bridge Engineering* 23 (9): 04018058. doi: [10.1061/\(ASCE\)BE.1943-5592.0001264](https://doi.org/10.1061/(ASCE)BE.1943-5592.0001264).
- Cornell, C. A., F. Jalayer, R. O. Hamburger, and D. A. Foutch. 2002. Probabilistic basis for 2000 SAC federal emergency management agency steel moment frame guidelines. *Journal of Structural Engineering* 128 (4): 526–33. doi: [10.1061/\(ASCE\)0733-9445\(2002\)128:4\(526\)](https://doi.org/10.1061/(ASCE)0733-9445(2002)128:4(526)).
- Du, A., and J. E. Padgett 2019. Multivariate surrogate demand modeling of highway bridge structures. In 12th Canadian conference on earthquake engineering, Quebec City, Canada, June, 8.
- Falamarz-Sheikhabadi, M. R., and A. Zerva. 2017. Analytical seismic assessment of a tall long-span curved reinforced-concrete bridge. Part II: Structural response. *Journal of Earthquake Engineering* 21 (8): 1335–64. doi: [10.1080/13632469.2016.1211566](https://doi.org/10.1080/13632469.2016.1211566).
- Gardoni, P., K. M. Mosalam, and A. Der Kiureghian. 2003. Probabilistic seismic demand models and fragility estimates for RC bridges. *Journal of Earthquake Engineering* 7 (spec01): 79–106. doi: [10.1080/13632460309350474](https://doi.org/10.1080/13632460309350474).
- Kawashima, K., and A. Mizoguti 2000. Seismic response of a reinforced concrete arch bridge. In 12th World Conference on Earthquake Engineering, Auckland, New Zealand.
- Kawashima, K., S. Unjoh, J. Hoshikuma, and K. Kosa. 2010. *Damage of transportation facility due to 2010 Chile earthquake*. Japan: Bridge Team Dispatched by Japan Society of Civil Engineers.
- Kulkarni, R., S. Adhikary, Y. Singh, and A. Sengupta, 2016. Seismic performance of a bridge with tall piers. In *Proceedings of the Institution of Civil Engineers-Bridge Engineering*, Vol. 169, No. 1, 67–75. Thomas Telford Ltd. doi:10.1680/bren.14.00027
- Lee, D. H., J. Park, K. Lee, and B. H. Kim. 2011. Nonlinear seismic assessment for the post-repair response of RC bridge piers. *Composites Part B: Engineering* 42 (5): 1318–29. doi: [10.1016/j.compositesb.2010.12.023](https://doi.org/10.1016/j.compositesb.2010.12.023).
- Liang, X., K. M. Mosalam, and S. Günay. 2016. Direct integration algorithms for efficient nonlinear seismic response of reinforced concrete highway bridges. *Journal of Bridge Engineering* 21 (7): 04016041. doi: [10.1061/\(ASCE\)BE.1943-5592.0000895](https://doi.org/10.1061/(ASCE)BE.1943-5592.0000895).
- Mangalathu, S., E. Choi, H. C. Park, and J. S. Jeon. 2018. Probabilistic seismic vulnerability assessment of tall horizontally curved concrete bridges in California. *Journal of Performance of Constructed Facilities* 32 (6): 04018080. doi: [10.1061/\(ASCE\)CF.1943-5509.0001231](https://doi.org/10.1061/(ASCE)CF.1943-5509.0001231).

- Mangalathu, S., F. Soleimani, J. Jiang, R. DesRoches, and J. E. Padgett 2017a. Sensitivity of fragility curves to parameter uncertainty using Lasso regression. In Proceedings of the 16th world conference on earthquake engineering, Santiago de Chile, Chile. Paper (Vol. 135).
- Mangalathu, S., F. Soleimani, and J. S. Jeon. 2017b. Bridge classes for regional seismic risk assessment: Improving HAZUS models. *Engineering Structures* 148: 755–66. doi: [10.1016/j.engstruct.2017.07.019](https://doi.org/10.1016/j.engstruct.2017.07.019).
- Mangalathu Sivasubramanian Pillai, S. 2017. Performance based grouping and fragility analysis of box-girder bridges in California. Doctoral diss., Georgia Institute of Technology.
- Mazzoni, S., F. McKenna, M. H. Scott, G. L. Fenves, and B. Jeremic. 2007. OpenSees command language manual. Pacific Earthquake Engineering Research Center. University of California, Berkeley.
- Nielson, B. 2005. Analytical fragility curves for highway bridges in moderate seismic zones. Doctoral diss., Georgia Institute of Technology.
- Padgett, J. E., and R. DesRoches. 2007. Sensitivity of seismic response and fragility to parameter uncertainty. *Journal of Structural Engineering* 133 (12): 1710–18. doi: [10.1061/\(ASCE\)0733-9445\(2007\)133:12\(1710\)](https://doi.org/10.1061/(ASCE)0733-9445(2007)133:12(1710)).
- Pang, Y., X. Dang, and W. Yuan. 2014. An artificial neural network based method for seismic fragility analysis of highway bridges. *Advances in Structural Engineering* 17 (3): 413–28. doi: [10.1260/1369-4332.17.3.413](https://doi.org/10.1260/1369-4332.17.3.413).
- Shome, N., C. A. Cornell, P. Bazzurro, and J. E. Carballo. 1998. Earthquakes, records, and nonlinear responses. *Earthquake Spectra* 14 (3): 469–500. doi: [10.1193/1.1586011](https://doi.org/10.1193/1.1586011).
- Simon, J., J. M. Bracci, and P. Gardoni. 2010. Seismic response and fragility of deteriorated reinforced concrete bridges. *Journal of Structural Engineering* 136 (10): 1273–81. doi: [10.1061/\(ASCE\)ST.1943-541X.0000220](https://doi.org/10.1061/(ASCE)ST.1943-541X.0000220).
- Soleimani, F. 2017. Fragility of California bridges-development of modification factors. Doctoral diss., Georgia Institute of Technology.
- Soleimani, F. 2020. Propagation and quantification of uncertainty in the vulnerability estimation of tall concrete bridges. *Engineering Structures* 202: 109812. doi: [10.1016/j.engstruct.2019.109812](https://doi.org/10.1016/j.engstruct.2019.109812).
- Soleimani, F. 2021. Analytical seismic performance and sensitivity evaluation of bridges based on random decision forest framework. In *Structures* (Vol. 32, pp. 329–341). Elsevier.
- Soleimani, F., B. Vidakovic, R. DesRoches, and J. Padgett. 2017c. Identification of the significant uncertain parameters in the seismic response of irregular bridges. *Engineering Structures* 141: 356–72. doi: [10.1016/j.engstruct.2017.03.017](https://doi.org/10.1016/j.engstruct.2017.03.017).
- Soleimani, F., C. S. W. Yang, and R. DesRoches. 2017b. The effect of superstructure curvature on the seismic performance of box-girder bridges with in-span hinges. In *Structures congress 2017: Bridges and Transportation Structures*, edited by J. G. Soules, 469–480. Reston, VA: ASCE.
- Soleimani, F., M. McKay, C. W. Yang, K. E. Kurtis, R. DesRoches, and L. F. Kahn. 2016. Cyclic testing and assessment of columns containing recycled concrete debris. *ACI Structural Journal* 113: 5. doi: [10.14359/51689024](https://doi.org/10.14359/51689024).
- Soleimani, F., S. Mangalathu, and R. DesRoches. 2017a. Seismic resilience of concrete bridges with flared columns. *Procedia Engineering* 199: 3065–70. doi: [10.1016/j.proeng.2017.09.417](https://doi.org/10.1016/j.proeng.2017.09.417).
- Soleimani, F., S. Mangalathu, and R. DesRoches. 2017d. A comparative analytical study on the fragility assessment of box-girder bridges with various column shapes. *Engineering Structures* 153: 460–78. doi: [10.1016/j.engstruct.2017.10.036](https://doi.org/10.1016/j.engstruct.2017.10.036).
- Song, J., and B. R. Ellingwood. 1999. Seismic reliability of special moment steel frames with welded connections: I. *Journal of Structural Engineering* 125 (4): 357–71. doi: [10.1061/\(ASCE\)0733-9445\(1999\)125:4\(357\)](https://doi.org/10.1061/(ASCE)0733-9445(1999)125:4(357)).
- Yashinsky, M., R. Oviedo, S. A. Ashford, L. Fargier-Gabaldon, and M. Hube, 2010. Performance of highway and railway structures during the February 27, 2010 Maule Chile earthquake. FHWA Bridge Team Report, EERI/PEER.
- Zhang, Y., Z. Yang, J. Bielak, J. P. Conte, and A. Elgamal 2003. Treatment of seismic input and boundary conditions in nonlinear seismic analysis of a bridge ground system. In 16th ASCE Engineering Mechanics Conference. Seattle, USA, University of Washington, July, 16–18.
- Zheng, Q. X., and W. H. Liu. 2010. Seismic design of high piers for mountain bridges. *ARPJ Journal of Engineering and Applied Sciences* 5 (9): 58–63.
- Zhong, J., P. Gardoni, D. Rosowsky, and T. Haukaas. 2008. Probabilistic seismic demand models and fragility estimates for reinforced concrete bridges with two-column bents. *Journal of Engineering Mechanics* 134 (6): 495–504. doi: [10.1061/\(ASCE\)0733-9399\(2008\)134:6\(495\)](https://doi.org/10.1061/(ASCE)0733-9399(2008)134:6(495)).